The Engine Performance, combustion, and Emission of Yellow Oleander (Thevetia peruviana) Biodiesel and Blends

Masime Jeremiah [*1], *Mbatia Betty* [2], *Ogur Erich* [3], *Aluoch Austin* [1], *and Otieno Geoffrey* [1]
[1]The Technical University of Kenya
[1] The School of Chemistry and Material Science,
[3]School of Mechanical and Manufacturing Engineering,
P.O. Box 52428 - 00200. Nairobi- Kenya.
[2]United States International University-Africa,
School of Pharmacy and Health Sciences

[*]Corresponding author; Email: : masimejo@yahoo.com.

Article Info

Article history:

Received October 20, 2022
Revised December 02, 2022
Accepted December 07, 2022

Keywords:

Yellow oleander biodiesel
Engine Load
Engine Performance
Combustion
Emissions

ABSTRACT (12 PT)

In this study, yellow oleander biodiesel was produced using a synthesized eggshell-derived nanocatalyst. Biodiesel fuel properties have been evaluated against a number of ASTM standards. A test was conducted in which an engine was fueled with petroleum diesel and four different petroleum diesel/biodiesel blends (B5, B15, B20, B30, and B100) at five different loads (0, 25, 50, 75, and 100 %) were analyzed in a single-cylinder internal combustion engine. Summaries of observations made from this work are reported. The lower calorific value decreased as the blend ratio increased and B100 had the lowest CV. Compared to petroleum diesel fuel, oleander yellow biodiesel had higher BTE, BSFC, and BP. The use of biodiesel resulted in lower emissions of CO and increased emissions of CO_2 and NO_x compared to petroleum diesel. This study showed that tailpipe emissions from diesel/biodiesel blends were lower than those from diesel fuels.

I. Introduction

An increase in demand for fossil fuels is a consequence of increasing industrialization and automation [1]. The global consumption of fossil heating oil is over 11 billion tons per year. Oil reserves will be depleted by 2042 as demand for crude oil has increased, causing reserves to fall by 4 billion tons per year [2], [3]. Approximately 88.6% of the global primary energy demand is covered by fossil fuels (Ashraful *et at*., 2014). Disadvantages of using coal, natural gas, and petroleum include volatile and unpredictable fuel prices [5]. The rapid proliferation of vehicles has led to a significant increase in exhaust emissions in emerging markets, resulting in an almost threefold increase in CO_2 emissions from the global vehicle fleet [6]. These emissions harm the environment and have a negative impact on the ozone layer, global warming, and greenhouse gas emissions. Anthropogenic greenhouse gases emitted into the atmosphere contribute to global climate change and generate El Niño, which produces recurrent and prolonged droughts [7], [8] and frequent and prolonged periods of drought [9]. It also causes health and safety problems [10], some incurable diseases [11][8], and the world's need to formulate sustainable and green policies [8], [12]. Solar power, wind power, geothermal power, tidal power, hydropower, and biofuels have all been identified as renewable energy sources [13].

A global energy transition is needed to limit the typical increase in global surface temperature to below 2 °C [14]. Carbon dioxide (CO_2) emissions from petrodiesel fuels represent a common contributor to greenhouse gases (GHG). The dynamic from fossil fuels to low-carbon fuels is expected to play an important role in reducing environmental emissions [15]. Using biodiesel significantly reduces warming and the atmospheric phenomenon [16]. Biodiesel is recognized as the number one carbon neutral fuel to reduce carbon dioxide emissions by 78% compared to diesel oil. In addition, biodiesel has a high biodegradability of 80.4% to 91.2% in 30 days, while fossil diesel is 24.5% (Supriyanto *et at*., 2021). It is environmentally friendly and sustainable, with similar combustion properties to petroleum diesel [18]. Another advantage of biodiesel is that its emissions are less harmful to the environment. Pure biodiesel, on the other hand, has a high oxygen content (approx. 11-15%). It promotes combustion by providing oxygen during combustion, reducing CO, HC, and PM emissions while slightly increasing NOx [19]. In addition, pure biodiesel has low sulfur dioxide emissions when burned in diesel engines because the sulfur content can be neglected [20]. Biodiesel has a higher cetane number (CN) and flash point (FP). Compared to petrodiesel, it is readily biodegradable and inherently lubricious [21]. However, the three main disadvantages of biodiesel are high raw material costs, low energy content, and high nit[21]rogen oxide (NOx) emissions.

Biodiesel is produced from transesterification reactions of edible and nonedible oils and can be used in diesel engines without engine modifications [22]. In addition, the viscosity of the biodiesel drops after transesterification so that it can be used directly in the engine. Other sources of biodiesel are animal fats and used cooking oils [23]. However, much biodiesel made from cooking oil is more expensive than petroleum diesel and is in direct competition with the food supply. As a result, studies on biodiesel production from various nonedible oilseeds have been conducted over the years, as they can reduce biodiesel production costs [24].

Most biodiesel is produced today by the transesterification of triglycerides of refined/edible type oils using methanol and an alkaline catalyst. The reaction is normally performed at 60–80 °C. The glycerol and biodiesel are separated by settling after catalyst neutralization. The crude glycerol and biodiesel obtained are then purified [25]. However, production costs are still rather high, compared to petroleum-based diesel fuel. There are two main factors that affect the cost of biodiesel: the cost of raw materials and the cost of processing. Although the homogeneously catalyzed process is relatively fast and shows high conversion, the associated bottlenecks were addressed by a heterogeneous catalyst. These bottlenecks include the energy-inefficient separation of the catalyst, the removal of by-products, the corrosive nature of the catalyst, and its reaction with FFA leading to the formation of soap. The use of heterogeneous catalysts could be an attractive solution [26].

Catalysts with heterogeneous bases have a number of advantages, including comparatively faster reaction rates, milder reaction conditions, lower energy consumption, easy separation from the reaction mixture, high probability of catalyst reuse and regeneration, and less corrosive properties [27]. Metal hydroxides, metal complexes, metal oxides such as zirconia, calcia, and magnesia, as well as zeolites, hydrotalcite, and supported catalysts are all part of the described heterogeneous catalyst chemistry. Because of its resilience, basicity, and complete solubility in alcohol, CaO is considered to be a superior heterogeneous catalyst [28]. Although thoroughly studied, the heterogeneous catalyst has lower reaction rates and causes undesirable side reactions such as saponification of glycerides and methyl esters and neutralization of free fatty acids by catalysts, which limits its use in industry [29].

Due to their large specific surface area, high catalytic efficiency, saponification resistance combined with good rigidity, nanocatalysts have become the focus for effective biodiesel production. In addition, the raw materials used to produce nanocatalysts should be non-hazardous, clean, and most importantly, affordable [30]. Chicken egg waste is recyclable, biocompatible, and has high catalytic efficiency. It is able to create a nanoporous structure and contains more than 90% $CaCO_3$. The use of nano-CaO based on egg waste and mollusk shells as heterogeneous catalysts for biodiesel application has been studied by a number of researchers. A biodiesel yield of 95% has been recorded for CaO made from apple snail shells and egg shells [31].

Various nonedible oil plants are found in nature all over the world. The nonedible oil feedstocks explored by researchers include *Ailanthus altissima*, *Azadirachta indica, Hevea brasiliensis*, *Hura crepitans*, *Jatropha curcas*, *Simmondsia chinensis*, *Madhuca indica*, *Nicotiana tabacum*, *Pongamia pinnata*, *Ricinus communis* and *Thevetia peruviana* [32]. *Thevetia peruviana* (Yellow oleander) seed has the highest oil content of ~ 60 – 67% of all the nonedible feedstocks for biodiesel production [33][34]. The present research considered the potential of yellow oleander oils for biodiesel production to replace reliance on edible oil feedstocks. According to a recent study, CaO is an effective heterogeneous catalyst for biodiesel synthesis. To our knowledge, no research has been conducted on the direct transesterification of yellow oleander using CaO nanocatalysts derived from eggshell waste. Engine performance, combustion, and emissions characteristics of the yellow oleander biodiesel and its blends with diesel of B5, B10, B15, B20, B30, and B100 were also evaluated. A single-cylinder, four-stroke, compression-ignition diesel engine was used without any modification.

II. Research Method

2.1. Preparation of the nanocatalyst

Waste chicken egg shells were collected from household waste, washed with warm tap water, and manually separated from the underlying membranes. It was then washed with distilled water and dried at 105°C for 1 hour. Then, the samples were crushed into powder and burned in a muffle furnace at 900°C for approximately 3 hours [35]. The resulting powder was reacted with 0.1 M aqua regia to form a mixture of calcium, magnesium, strontium, copper, chromium, iron, titanium, and zinc nitrates.

Two different microemulsions, A and B, were used for the synthesis of eggshell nanocatalysts. Microemulsion A (25 cm^3) was prepared by adding 2.5 cm^3 of 0.1 M aqueous eggshell solution containing, inter alia, calcium, magnesium, strontium, copper, chromium, iron, titanium, and zinc nitrate 3.5 cm^3 n-butanol as a cosurfactant, 15 cm^3 iso-octane as a nonpolar solvent and 4.20 g cetyltrimethylammonium bromide (CTAB) as a surfactant. Microemulsion B (25 cm^3) was prepared by adding 2.5 cm^3 of 0.1 M aqueous ammonium carbonate solution, 3.5

cm^3 of n-butanol as a cosurfactant, 15 cm^3 of isooctane as a nonpolar solvent, and 4.20 g of cetyltrimethylammonium bromide (CTAB) as a surfactant. The microemulsions (A and B) were first stirred, poured into a single container and stirred overnight with a magnetic stirrer. To stabilize the suspension formed, it was stirred at 700 rpm for 24 hours. The residue separated from the microemulsion after centrifugation. It was washed with a 1:1 mixture of chloroform and methanol, dried at room temperature and then incinerated at 900°C [36] for three hours to produce the nanocatalyst.

2.2. Transesterification of yellow oleander oil

2.2.1. Catalyst activation with methanol

Before using the synthesized nanocatalyst in biodiesel production, it was necessary to activate it. First, the nanocatalyst was activated with methanol at room temperature for 1 h in a conical flask with a magnetic stirrer at 650 rpm. This activation was necessary to produce calcium methoxide to initiate the transesterification reaction.

2.2.2. Yellow oleander biodiesel production

The transesterification reaction was carried out in a 250 ml conical flask using the temperature-controlled magnetic stirrer. In a typical experimental run, 50 g of the yellow oleander oil was measured into the conical flask and preheated to the desired temperature using the magnetic stirrer. This research studied the effects of the following parameter: methanol/oil molar ratio (3:1 to 7:1), catalyst loading (1 to 5%), reaction temperature (30 to 80 °C), reaction time (30min. to 180min), and reusability of catalyst (1 to 5 times) on the conversion to biodiesel. A known weight of synthesized nanocatalyst was dissolved in the methanol while stirring gently at room temperature to allow for complete dissolution with minimal methanol evaporation. Then methoxide mixture was added to the preheated oil. The stirrer and temperature control were also turned on to start the reaction. After the reaction, the mixture was separated from the catalyst by decantation and filtration. The mixture was later transferred to a separating funnel and allowed to settle overnight; it can be left for 2 days to get better results. After the 24hrs period, the reaction result was in two distinct liquid phases; the first was the yellow oleander biodiesel on the top, and the second was the denser phase of glycerol. The two phases were separated using a separating funnel. The biodiesel layer was showered with cold or warm deionized water several times until it became clean to remove any traces of methanol, glycerol, catalyst, and water. After that, the washed biodiesel was placed in an oven and heated to 80 °C to remove water that might still be present in the biodiesel. The drying continued until no traces of water droplets were noticed at the lower layer of the biodiesel. Finally, the dried yellow oleander biodiesel was weighted for yield calculations, and the biodiesel yield was analysed. The biodiesel yield was obtained using the equation:

$$Biodiesel\ yield(\%) = \frac{mass\ of\ biodiesel\ (g)}{massof\ \ yellowoleander\ oil} \times 100 \ldots.. 2.2.2.1.$$

2.2.3. Catalysts characterization

The nanocatalyst was characterized by X-ray fluorescence (XRF), Transmission electron microscopy (TEM), and Brunauer-Emmer-Teller (BET) surface area. Chemical compositions Chemical compositions were analysed using X-ray fluorescence (XRF) (Philips, model PW 2400) at a tube current of 1000 A with an acquisition lifetime of 30 s [37]. For transmission electron microscopy (TEM) analysis, samples were prepared by placing a drop of the nanoparticle suspension on a copper grid (Ted Pella, CA) and air drying it overnight. TEM imaging was done using a JEOL 123 microscope operated at 80 kV (JEOL, USA) [38] [39]. BET (Brunauer, Emmett, and Teller) surface area of the catalyst samples was obtained using a Micromeritics TriStar 3000 Surface Area and Porosity System analyzer low-temperature N_2 adsorption method. Before analysis, the samples were degassed at 120°C overnight (12 h) under a continuous flow of N_2 gas to remove the adsorbed contaminants and moisture from the material's surface and pores [40]. This research used the ASTM C1274-12 Standard Test Method for Advanced Ceramic Specific Surface Area by Physical Adsorption [41].

2.2.4. Properties of yellow oleander oil and biodiesel

The study evaluated the quality of yellow oleander oil and biodiesel using the requirements of the American Society for Testing and Materials (ASTM D-6751), American Oil Chemists Society (AOCS) Cd 8-53, 8-53 and the International Organization for Standardization (ISO) requirements. Among the fuel (ISO). The examined fuel properties included the cetane number, specific gravity, kinematic viscosity, saponification value, number, acid value, number, peroxide value, number, iodine value, flashpoint, number, flash point, and pour point. The following standards were used in the tests: ASTM D 1962, D 664, D 1563, D 127, D 445, D 613, D 93, D 287, D 97, AOAC 993.20, 20 and AOCS 1d – 92 [42] [43].

2.2.5. Biodiesel-Diesel Blend

Diesel and biodiesel test blends (B5, B10, B15, B20, B30, and B100) were prepared on a v/v% basis and used in a diesel engine to evaluate engine performance. In a 1-liter volumetric flask, required volumes of diesel and biodiesel were added and mixed to obtain the different blends. A total of 50 cm^3 (5%) pure yellow oleander biodiesel or petrodiesel was measured and thoroughly mixed with 950 cm^3 (95%) petrodiesel to make a 1 liter B5 blend. The B10 blend consisted of 900 cm^3 (90%) petroleum diesel and 100 cm^3 (10%) undiluted yellow oleander biodiesel. The B20 blend was produced by combining 800 cm^3 (80%) fossil diesel and 200 cm^3 (20%) virgin yellow oleander biodiesel.

2.2.6. Engine Performance Analysis

The test setup shown in Figure 1 includes all the equipment required to measure the various engine parameters.

Figure 1: Photograph of the experimental setup

To feed the load at various operating conditions, the motor used an eddy current type dynamometer. They were placed on a shared concrete bed. The frame construction was isolated from the concrete using a vibration-damping fastening method. These engines are designed to allow compression ratio (CR) modulation even while the engine is running. An attached micrometer was used to measure cylinder movement. Piezo sensors were installed on the cylinder head and fuel injector to regulate combustion pressure and fuel flow. To ensure that exhaust gas and leaving cooling water temperatures were constant and the variable compression ratio (VCR) engine was able to reach a steady state, it was initially run on diesel fuel and at full load for the first 20 minutes. This indicated that the in-cylinder combustion process had stabilized and the engine was ready to begin data collection. The engine then ran for five minutes, gradually returning to idle. In order to stabilize the system before starting the experiment to measure the emissions, and flue gas analyzer was also switched on for a short time.

All data were taken under steady-state conditions after the engine was started with no load and 25%, 50%, 75%, and 100% loading conditions at 2-minute intervals. Diesel fuel is used to start the engine and is then allowed to warm up for approximately 10 minutes with no load. The tests were conducted with diesel fuel only while the engine was running at different engine speeds of 500, 750, 1000, 1250, and 1500 rpm. This data represented the engine braking forces at CRs 16:1, 17:1, and 18:1. The other experimental parameters including engine speed, IT, and IP were maintained at 1500 rpm, 23° bTDC, and 210 bar throughout, as such values were assumed to be typical of the VCR engine used. After the diesel tests, CRs of 16:1, 17:1, and 18:1 were used to evaluate yellow oleander biodiesel blends (B5, B10, B15, B20, B30, and B100), with 17:1 serving as the standard CR. The engine was allowed four minutes to settle before any data were collected at the test speed and engine load, and ICEngineSoft Version 9.0 software was used to calculate the results.

2.2.6.1. Engine Specifications

All tests were performed after the thermal stabilization of the engine. Table 1 lists the engine specifications.

Table 1: Engine Specifications

Engine Name	**Research Diesel**
Engine type	Vertical, 4-stroke, compression ignition engine Model DM-10, constant speed, direct injection, single cylinder, and water cooled
Rated power	3.5 kW at 4000 rpm
Bore/stroke	110 (mm)
Swept Volume (cc)	661.452
Compression ratio	17.5:1
Cylinder Bore (mm)	87.5
Connecting Rod Length (mm)	234
Start of fuel injection	26° bTDC
Nozzle opening pressure	200– 205 bar
BMEP at1500 rpm	6.34 bar

All the fuel samples were tested with the 4-stroke engine under the above conditions. The engine was run for at least three minutes under each load situation before data were collected. Three replicates of the experiment were performed. Emission values were recorded in triplicate for each setting, and their average was used as a benchmark. Brake efficiency (BTE), brake specific fuel consumption (BSFC), brake power (BP), exhaust gas temperature, cylinder pressure (pc), rate of pressure rise $\left(\frac{dp}{d\theta}\right)$, net heat release rate $\left(\frac{dQ_n}{d\theta}\right)$, and emissions of carbon monoxide (CO), carbon dioxide (CO_2), unburned hydrocarbons (HC) and nitrogen oxides (NOx) with exhaust gas opacity were used to evaluate engine performance under different loads and operating conditions.

In the combustion analysis of yellow oleander biodiesel and its blends, the cylinder pressure was measured with a Kistler 6058A piezoelectric sensor, and its signal was recorded with a high-speed data acquisition system. The pressure sensor was installed in the head of the first cylinder using a glow plugs adapter. The charge signal from the pressure sensor was amplified by a Kistler charge amplifier. The angle of the encoder was adjusted to a resolution of 0.125 crank angles using a Leine & Linde incremental encoder (CA). Cylinder pressure readings were recorded for each test and averaged over 100 consecutive cycles.

The exhaust gases were sampled from the exhaust line using a specially designed arrangement that diverted the exhaust gas to a sampling line without increasing the back pressure, and the exhaust gas concentration was measured using an MRU DELTA 1600-V gas analyser. The following gases are measured: carbon monoxide (CO), carbon dioxide (CO_2), hydrocarbons (HC), and nitrogen monoxide (NOx). With an accuracy of 1.12% and a sensitivity of 16.5 pc/bar, the Kistler 601A piezoelectric pressure transducer was used to measure the in-cylinder pressure from 0 to 250 bar. The pressure sensor was connected to a Nexus charge amplifier type 2692-A-0S4. The piston top dead center was measured using a model LM12-3004NA proximity switch (TDC). The average cylinder pressure was recorded over 125 engine cycles. Through the LABVIEW software connected to the PC, the NI-USB-6210 data acquisition board collected the sensor data.

III. RESULTS AND DISCUSSION

3.1. Physical and chemical characteristics of yellow oleander oil, biodiesel and blends

Table 1 gives the physical-chemical and fuel properties of yellow oleander oil (YOO) and yellow oleander biodiesel using the ASTM (D6751) specifications. Some of the properties are compared with those of petrodiesel.

Table 1: Physical and chemical characteristics of yellow oleander oil, biodiesel and blends

	YOO	**B100**	**B30**	**B20**	**B15**	**B10**	**B5**	**ASTM**
SG	0.88	0.86	0.84	0.83	0.82	0.81	0.81	0.86-0.90
KV at (40 °C) cSt	24.4	4.86	5.5	5.21	4.67	4.33	4.2	1.9 - 6.0
CN	48	47.6	58.3	50.1	49.6	49.1	48.7	47 min.
FP °C	146	168	140	138	145	150	155	130 Min
CV MJ/Kg	43.2	41.9	42.8	43.2	43.6	44.1	44.50	>35.00
API	22.3	29.3	36.3	38.9	41.1	43.2	43.2	36.95

3.1.1. Specific gravity

In this study, the specific gravities of petrodiesel, yellow oleander biodiesel, and oil were 0.83 ± 0.03, 0.86 ± 0.06, and 0.88 ± 0.1, respectively. In the same study the specific gravities of the biodiesel blend B30, B20, B15, B10, and B5, were found to be 0.84, 0.83, 0.82, 0.82, 0.81, and 0.81 respectively. They were within the allowed ASTM D6751 range of 0.82 to 0.90, proving that the biodiesel, the oil, and the blends were pure substances. The results showed that as the biodiesel content in the blends increased, so did the specific gravity values. This can lead to improved lubricity. Ighose *et at.*, (2017) obtained similar results when studying the specific gravity of biodiesel from yellow oleander. They discovered that the specific gravity of biodiesel was 0.89, consistent with literature values for biodiesel ranging from 0.87 to 0.89. High-density biodiesels are preferred because they provide more fuel

3.1.2. Kinematic viscosity

The kinematic viscosity of petrodiesel, yellow oleander biodiesel and oil were; 2.9, 4.86, and 24.4 $mm^2 s^{-1}$, respectively. In the same study the kinematic viscosity of the biodiesel blends B30, B20, B15, B10, and B5, were found to be 5.5, 5.21, 4.67, 4.33, and 4.2 respectively. Accordingly, the kinematic viscosity values also increased with increasing biodiesel content of the mixtures, which led to improved lubricity. These were within the limit of ASTM D6751 standard of 1.9- 6.0 $mm^2 s^{-1}$ though much higher than petro-diesel, confirming that yellow oleander biodiesel and blends can be used in a diesel engine. Ighose *et at.*, (2017) obtained similar results when studying the kinematic viscosity of yellow oleander oil and biodiesel. They found that the yellow oleander oil had a high kinematic viscosity of 57.73 $mm^2 s^{-1}$ compared to the literature value of 35.47 $mm^2 s^{-1}$ obtained after the transesterification reaction.

3.1.3. Cetane number

The cetane numbers of petrodiesel, yellow oleander biodiesel, and oil were 41, 47.6, and 48, respectively. In the same study, the cetane numbers of biodiesel blend B30, B20, B15, B10, and B5 were found to be 58.3, 50.1, 49.6, 49.1, and 48.7, respectively. These were within the limit of ASTM D6751 standard of > 47 though much higher than petro-diesel. This confirms that yellow oleander biodiesel and blends can be used in a diesel engine. It was found that the cetane number (CN) decreased with increasing biodiesel content in the blends. However, according to this study, the ASTM cetane number for biodiesel blends, with the exception of B100 and B30, was within the ASTM range of 4751, although higher than that of petrodiesel [44]. Ighose *et at.*, (2017) obtained similar results when examining the cetane number of yellow oleander oil and biodiesel. They observed cetane numbers of 59.54 and 125.74 for oil and biodiesel, respectively. These values were above the ASTM standard of 47 minutes, indicating good ignition and combustion properties of the fuel.

3.1.4. Flash point

The flash points for petrodiesel, biodiesel, and yellow oleander oil were; 53, 168, and 146, respectively. In the same study, the flash points of biodiesel blend B30, B20, B15, B10, and B5 were found to be 140, 138, 145, 150, and 155, respectively. Flashpoints of the biodiesel blends increased with increasing biodiesel content in the blends. This requires improved handling and safety during transportation, transportation, and storage. These values were above the ASTM lower limit of 130, proving that the oil Biodiesel and blends can be used in a diesel engine. Other research shows that the flash points of vegetable oils and biodiesel are always higher than those of petrodiesel [44]. Although generally, fuels with a flash point above 66 ºC are considered safe, biodiesel fuel is more secure to handle than petrodiesel [45]. Yarkasuwa *et at.*, (2013) obtained similar results when investigating the flash points of yellow oleander biodiesel. They observed that the flash points of the methyl and ethyl esters of yellow oleander were 175 and 198°C, which was above the ASTM range of 100-170. Due to the higher flash point, yellow oleander biodiesel has a low tendency to cause fire hazards. As a result, it has certain advantages over petroleum, such as excellent safety in storage, handling, and transport.

3.1.5. Calorific value

The calorific values of petrodiesel, yellow oleander biodiesel, and oil were; 46, 41.9, and 43.2 MJ kg^{-1}. In the same study, the flash points of biodiesel blend B30, B20, B15, B10, and B5 were found to be 42.8, 43.2, 43.6, 44.1, and 44.5 MJ kg^{-1}, respectively. It was found that the calorific value (CV) decreased with increasing proportion of biodiesel in the blends. These values have been found to be within the ASTM limit of 33-40 kJ kg^{-1}. Adepoju *et at.*, (2018) came to similar conclusions when examining the higher heating value (HHV) of yellow oleander oil and biodiesel. They discovered that the calorific values of biodiesel and yellow oleander oil were 47.056 and 45.34 kJ kg^{-1}, respectively, which included the latent heat of vaporization of water in the combustion products.

3.1.6. American Petroleum Index (API)

The API index of petrodiesel, biodiesel, and yellow oleander oil were; > 30, 43.2, and 22.3. In the same study, the API index of biodiesel blend B30, B20, B15, B10, and B5 were found to be 43.2, 41.1, 38.9, 36.9, and 29.3, respectively. These values have been found to be within the ASTM limit of greater than 30. Adepoju *et at.*, (2018) obtained similar results studying the API of yellow oleander oil and biodiesel. They observed that the API value decreased by 10.71% from 27 in yellow oleander oil to 23.48 in biodiesel, these values were below the ASTM recommended minimum of 30. As a result, the study confirmed that the yellow oleander oil produced by biodiesel could serve as an alternative to conventional diesel and its blends could improve fuel properties.

3.1.7. Diesel Index (DI)

The diesel index of petrodiesel, yellow oleander biodiesel, and oil were; 59.8, 54, and 53. In the same study, the diesel index of biodiesel blend B30, B20, B15, B10, and B5 were found to be 54.6, 55.4, 66.7, 51.9, and 52.5, respectively. These values were above the ASTM limit of 50.4. It was found that the diesel index (DI) decreased with increasing petroleum diesel content in the blends. Adepoju *et at.*, (2018) obtained similar results studying the diesel index of biodiesel from yellow oleander. They found that the diesel index of the biodiesel was 87.40, which is higher than that of petrodiesel, and the results are comparable to those obtained by other researchers using biodiesel from different oilseeds.

Yellow Oleander biodiesel's physicochemical and fuel properties was within the ASTM D6751 standards. Additionally, it was noted in the report that the biodiesel produced possessed qualities that were consistent with those described in the literature. Consequently, the yellow oleander plant makes a suitable feedstock for making biodiesel.

3.2. Engine Performance Analysis

Performance, combustion, and emission characteristics of biodiesel-diesel blends of B5, B10, B15, B20, B30, and B100 on indirect injection engines operating under different loads at 1500 rpm were evaluated.

3.2.1. Performance characteristics

3.2.1.1. Variation in brake thermal efficiency with load

The variation in brake thermal efficiency with load is given in Figure 2.

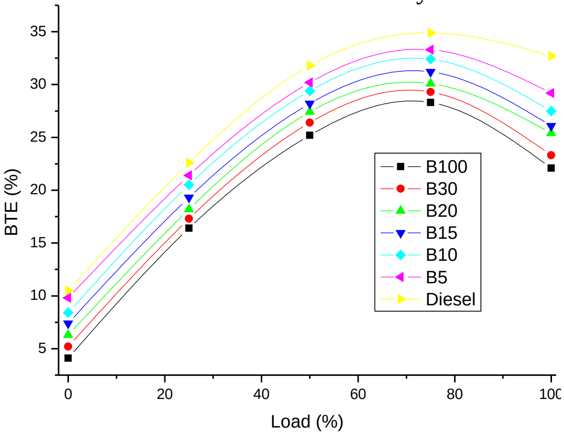

Figure 2: Variation in brake thermal efficiency with load

The brake thermal efficiency of all blends was directly proportional to the brake thermal efficiency of petrodiesel. BTE for petrodiesel at full load condition was 35.14%, whereas for the blends B5, B10, B15, B20, B30 and B100 were 28.19 %, 29.39 %, 30.97 %, 32.08%, 33.06 % and 33.61 % respectively. Blends of biodiesel have brake thermal efficiency lower than petrodiesel. Arun *et at*., (2018) obtained similar results analyzing the performance of yellow oleander biodiesel in compression ignition (CI) engines. In their study, they found that B30 had a lower BTE of 28.11% than B100, which recorded 27.31%, while the BTE of pure petrodiesel was 31.68%. They also observed that, in general, the BTE decreased with increasing concentration of yellow oleander biodiesel in the blends, but the BTE increased with increasing load. This was due to an increase in fuel consumption, which increases the BTE. Among the test fuels, the BTE values of all biodiesel-petrodiesel blends were lower than the petrodiesel values at all load conditions. This has been attributed to the high calorific value of petroleum diesels, which results in high energy release due to combustion.

3.2.1.2. Brake Specific Fuel Consumption

Brake Specific Fuel Consumption is the rate of fuel consumption divided by the power produced. Figure 3 shows the variation in BSFC against engine load.

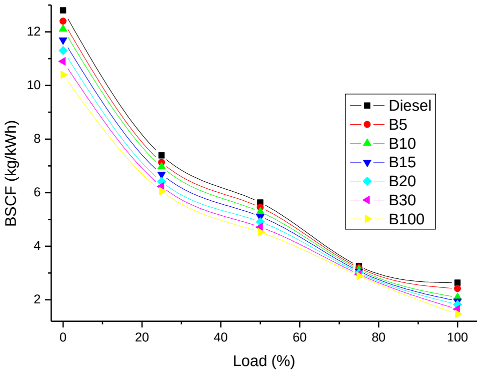

Figure 3: Variations in brake specific fuel consumption and engine load

The BSFC decreased as the load increased, while B100 recorded the highest BSFC. This revealed that with the increase in yellow oleander biodiesel in the blend, the BSFC increased. However, the BSFC of blends B5, B10, B15, B20, B30, and B100, results were similar to those recorded for petrodiesel. Over the full load range, yellow oleander biodiesel and its blends demonstrated greater BSFC than petrodiesel. When compared to petrodiesel, in B100 the BSFC increased by 48.38% at 100% engine load and by 15.99% at 80% engine load. B20 demonstrated an increase of 7.64 % and 45.59 % at the engine loads 80% and 100% respectively. Arun *et at.*, (2018) obtained similar results by analyzing the performance of yellow oleander biodiesel in compression ignition (CI) engines. In their study, they found that the BSFC of all test fuels was 0.3 kg kW^{-1} h^{-1}, while for petrodiesel it was 0.28 kg kW^{-1} h^{-1}. In their study, B30 showed less BSFC compared to B100, while for petrodiesel, BSFC was less than B100. They also observed for all test blends that BSFC decreased with increasing exposure. This was because biodiesel has a calorific value that is 37.56 MJ kg^{-1} lower and a lower energy density than petrodiesel, which means that more fuel is used for the same engine power. It has also been noted that as the proportion of biodiesel in the blends increased, the calorific value of the blend decreased due to the lower calorific value compared to petrodiesel [46].

3.2.2. The emission characteristics

3.2.2.1. Carbon dioxide (CO_2) emissions

Figure 4 shows the variation in carbon dioxide of petrodiesel, yellow oleander biodiesel (B100), and biodiesel blends (B5, B10, B15, B20, and B30).

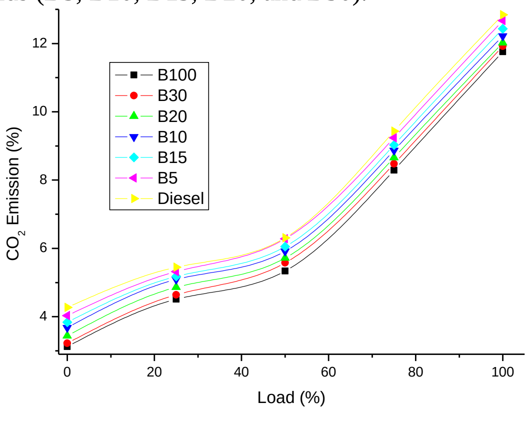

Figure 4: Variations in CO_2 with engine load

For all fuel modes, the CO_2 emissions increased with the load up until a maximum loading stage of 100%. The maximum loading value for CO_2 emissions using petrodiesel was 12.9%, while the minimum loading value for CO_2 emissions using all biodiesel fuel blends was 3.1%. It was also observed that as the biodiesel component in the biodiesel blends rose, so did the CO_2 emission. For B 100, there were lower carbon dioxide levels due to better fuel atomization and complete fuel combustion. Arun *et at.*, (2018) obtained similar results by analyzing the performance of yellow oleander biodiesel in compression ignition (CI) engines. In their study, they found that the blends B10, B20, and B30 had the highest CO_2 emissions of all fuels examined. The CO_2 emissions of B40 and

B30 in oleander-biodiesel-petrol-diesel blends were high and 8.05% higher than the CO_2 emissions of diesel. At 100% load, the CO_2 emissions of petrodiesel and yellow oleander biodiesel are 8.7% and 9.4%, respectively.

3.2.2.2. Emission of CO

The emissions of carbon monoxide (CO) indicate incomplete fuel combustion inside the engine cylinder. Emissions of CO, HC, and PM increase when fuel combustion rates decrease [43]. Figure 5 shows the variation in CO of petrodiesel, yellow oleander biodiesel (B100) and blends of B5, B10, B15, B20, and B30.

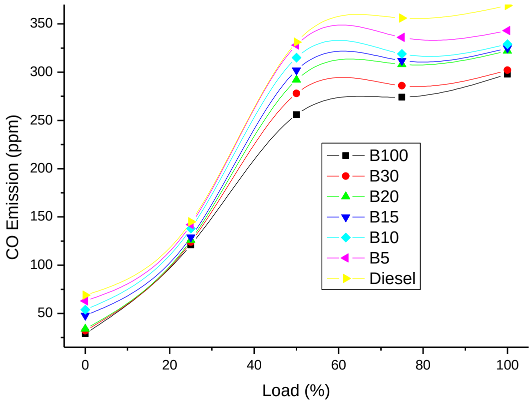

Figure 5: Variation in CO emissions with load

For all fuel modes, the CO emissions increased at higher loads. At low and medium loads, the carbon monoxide emissions of the biodiesel fuel blends were not significantly different from those of petrodiesel; however, at maximum load, CO decreases significantly in comparison to diesel fuel. This is because biodiesel blends have a higher oxygen content, which will encourage the oxidation of the CO during the exhaust process. The petrodiesel fuel has a CO content of 366 ppm at full load, compared to 298, 302, 319, 320, 328, and 344 ppm for B100, B30, B20, B15, B10 and B5 biodiesel blends. As a result, when compared to pure diesel fuel, the biodiesel blends cut CO by 0.34 % to 6 % at full load. Rath *et at.*, (2011) obtained similar results for the CO emission analysis for Karanja methyl ester (KME). They observed that almost all KME biodiesel blends had slightly lower CO emissions. The presence of oxygen in the fuel improved the combustion properties of the fuel. At higher temperatures during combustion in the combustion chambers and at higher loads, the fuel burns more effectively and more completely, producing very little carbon monoxide.

3.2.2.3. Emission of NO_x

Figure 6 shows the NOx emissions for all the yellow oleander blends and petrodiesel fuel.

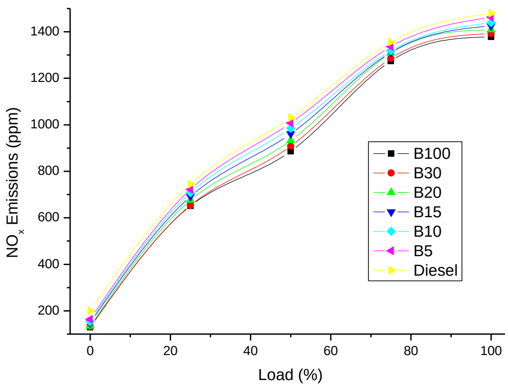

Figure 6: Variation in NO_x emissions with load

The NOx emissions from all biodiesel blends are lower than those from petrodiesel fuel under all load circumstances. All biodiesel blends exhibited a complete reduction in NOx output. At full load conditions, the NOx emissions of the biodiesel blends B100, B30, B20, B15, B10, B,5 and petrodiesel are 1378, 1392, 1409, 1425, 1439, 1463 and 1480 ppm, respectively. The decreased NOx emission is due to the greater cetane number of yellow oleander oil. Higher cetane number fuels have a shorter premixed combustion time due to a shorter ignition delay.

This predicts a slower rise in combustion pressure, which leads to lower temperatures and a slower rate of NOx generation. The emission NOx emission increased with decreasing biodiesel content in the blends. This was due to increased volumetric efficiency and gas flow motion within the engine cylinder [21]. Shirneshan (2013) obtained similar results for the NOx emission analysis for used frying oil methyl ester. They observed that the NOx concentration increased with increasing engine load for all fuels. Compared to petrodiesel, the NOx emission of the fuel blended with biodiesel increased slightly at all engine loads tested, and the increase was more pronounced at higher engine loads.

3.2.3. Combustion analysis

3.2.3.1. The variation in combustion pressure

The variation of the instantaneous heat release rate (HRR) with crank angle for petroleum-based and biodiesel blends (B5, B10, B15, B20, B30, and B100) under conditions of full load is shown in Figure 7. This was accomplished by injecting at 100% load and 25° before the top dead center (bTDC).

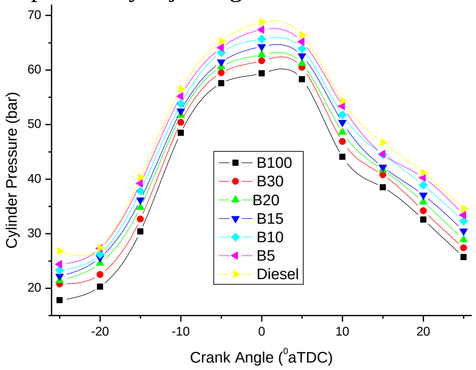

Figure 7: Variation in cylinder pressure with crank angle at 100% load

Before and after the 25° crank angle, the cylinder pressure for biodiesel-diesel fuel was proportional to petrodiesel. For tested fuels, the highest pressure appeared between -4.96° and 5.39° after TDC (aTDC). Petrodiesel showed a max cylinder pressure of 68.48 bar at 0.12° aTDC. When compared to petrodiesel peak pressure, biodiesel blends had lower peak cylinder pressure. This is because biodiesel-based diesel fuels have a shorter delay time. The higher cetane number, high oxygen concentration, and earlier start of combustion for biodiesel-diesel blends compared to petrodiesel are the reasons for the shorter delay period. The pressure rises for biodiesel-diesel blends is lower than petrodiesel, from -5.1° bTDC to 5.2° aTDC. This is as a result of their higher cetane number and lower calorific value when compared to diesel. According to results from the B100 test fuels, the cylinder pressure peaked at a high 69.01 bar (2.22°). For all tested fuels, the highest peak cylinder pressure obtained for B5 was 2.17%, and less than petrodiesel peak cylinder pressure. The lowest peak cylinder pressure was obtained for B100, which was 12.1% less than petrodiesel peak cylinder pressure. In the combustion analysis of yellow oleander biodiesel, with the exception of between 350° and 375° crank angles. Arun *et at.*, (2018) obtained similar results for studying the combustion parameter for yellow oleander biodiesel on a compression ignition (CI) engine. They observed that the pressure increases for biodiesel-diesel fuels from 5 bTDC to 10 aTDC is less than for petrodiesel. This is due to the higher cetane number and lower calorific value compared to petroleum diesel. The maximum cylinder pressure for B30 test fuels was high at 71.076 bar (8). B30, which is 0.93% lower than diesel, was identified as the test fuel with the highest peak cylinder pressure. B100 had the lowest peak cylinder pressure, which was 7.42% lower than the peak cylinder pressure for petrodiesel.

3.2.3.2. Heat release rate

The heat release rates (HRRs) of diesel, yellow oleander biodiesel (B100), (B5, B10, B15, B20, and B30) biodiesel blends are presented in Figure 7.

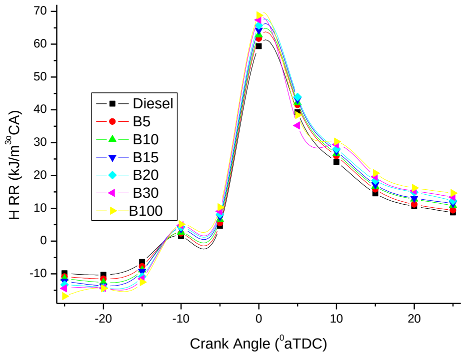

Figure 8: Variation in the heat release rate with crank angle at 100% load

In comparison to biodiesel mixes, diesel has a larger heat release during premixed combustion (69.22 kJ/m^3-deg). All blends release heat at a slower pace compared to petrodiesel fuel. Blends B5, B10, B15, B20, B30, and B100 had maximal heat transfer rates of 60.35, 65.87, 63.49, 63.98, 60.63, and 60.36 kJ m^3-deg, respectively. The high viscosity of biodiesel and blends led to poor atomization of fuel droplets. This resulted in poor combustion, hence less HRR for B100. The oxygen present in the biodiesel blends, promotes better combustion and a greater peak heat release rate. B5 recorded the highest peak heat release rate during the combustion phase. Arun *et at.*, (2018) obtained similar results for studying the combustion parameter for yellow oleander biodiesel on a compression ignition (CI) engine. They found that high viscosity leads to poor atomization of fuel droplets, resulting in poor combustion, which is why less HRR was obtained for B100. Among the biodiesel blends, B30 showed a higher HRR due to the high O_2 content of B30, resulting in complete combustion that increased the HRR compared to B10 and B20.

IV. CONCLUSION

Yellow oleander biodiesel was generated in this study using a transesterification reaction and an eggshell-derived nanocatalyst. The physicochemical properties, engine performance, combustion and emission properties of mixed yellow oleander biodiesel, pure biodiesel and petrodiesel in a CI engine were studied. The results of the determinations are recorded in this report.

V. ACKNOWLEDGEMENT

The authors would like to thank the Technical University of Kenya, the Kenya Industrial Research and Develop-ment Institute, and the Jomo Kenyatta University of Agriculture and Technology for providing their research laboratories for this work. This work was supported in part by a grant from the Kenya National Research Funds (NRF), 2017/2018.

References

[1] Adepoju, T. F., Olatunbosun B. E., Olatunji O. M., and Ibeh M. A. 2018, "Brette Pearl Spar Mable (BPSM): A Potential Recoverable Catalyst as a Renewable Source of Biodiesel from Thevetia Peruviana Seed Oil for the Benefit of Sustainable Development in West Africa." *Energy, Sustainability and Society* 8 (1): 1–17.

[2] Arun, S. B., Suresh R., and Yatish K.V. 2018, "Study of Performance, Combustion and Emission Characteristics of Heterogeneous Catalyzed Yellow Oleander Biodiesel on Compression Ignition (CI) Engine" *Biofuels*.7269:1–8

[3] Ashraful, et al, "Production and Comparison of Fuel Properties, Engine Performance, and Emission Characteristics of Biodiesel from Various Non-Edible Vegetable Oils: A Review." *Energy Conversion and Management* 80: 202–28.

[4] Ayodeji A.A., Ojewumi M.E., Rasheed B., and Ayodele J.M. 2018, "Data on CaO and Eggshell Catalysts Used for Biodiesel Production." *Data in Brief* 19: 1466–73.

[5] Carlucci C. 2022, "An Overview on the Production of Biodiesel Enabled by Continuous Flow Methodologies." *Catalysts*.12(7), 717:1-31.

[6] Chinthakuntla A., Venkateswara R. K, Ashok C., Dayakar T. and Kiran K. M. 2014. "Calcium Oxide Nano Particles Synthesized from Chicken Egg Shells by Physical Method," International Conference on Emerging Technologies in Mechanical Sciences. 72-75.

[7] Damanik N., Ong H.C., Chong W.T., and Silitonga A.S. 2017, "Biodiesel Production from Calophyllum Inophyllum–palm Mixed Oil." *Energy Sources, Part A: Recovery, Utilization and Environmental Effects* 39 (12): 1283–89.

[8] Datta A., and Mandal B.K.. 2014, "Use of Jatropha Biodiesel as a Future Sustainable Fuel." *Energy Technology & Policy* 1 (1): 8–14.

[9] Demirbas A., Bafail A., Ahmad W., and Sheikh M. 2016, "Biodiesel Production from Non-Edible Plant Oils." *Energy Exploration and Exploitation* 34 (2): 290–318.

[10] Ji Y. 2019, "Recent Development of Heterogeneous Catalysis Catalysis in in the Transesterification Transesterification of of Glycerol Glycerol to to Glycerol." *Catalysts,* 9, 581:1-23.

[11] Diamantopoulos N. 2015, "Comprehensive Review on the Biodiesel Production Using Solid Acid Heterogeneous Catalysts." *Journal of Thermodynamics & Catalysis* 06 (01). *1-8.*

[12] Dominic O., Joseph E., Callistus U., and Kenechi N. 2022, "Improving Heterogeneous Catalysis for Biodiesel Production Process." *Clean Chem Eng 3:100038: 1-10.*

[13] Gaide I., Makareviciene V., and Sendzikiene E. 2022, "Effectiveness of Eggshells as Natural Heterogeneous Catalysts for Transesterification of Rapeseed Oil with Methanol." *Catalysts*. 12: 246: 1-13.

[14] Ge J.C., Yoon S.K., and Song J.H. 2021, "Comparative Evaluation on Combustion and Emission Characteristics of a Diesel Engine Fueled with Crude Palm Oil Blends." *Applied Sciences (Switzerland)* 11 (23).11502: 1-16.

[15] Ge J., Yoon S., and Choi N. 2017, "Using Canola Oil Biodiesel as an Alternative Fuel in Diesel Engines: A Review." *Applied Sciences* 7 (9): 881:1-19.

[16] Gebremariam S., Marchetti J.M. 2018, "Economics of Biodiesel Production: Review." *Energy Conversion and Management* 168 (May): 74–84.

[17] Gielen D., Boshell F., Saygin D., Bazilianc M. D., Wagner N., and Gorini. 2019, "The Role of Renewable Energy in the Global Energy Transformation." *Energy Strategy Reviews* 24 (June 2018): 38–50.

[18] Guo S., Yang Z., and Gao Y. 2016, "Effect of Adding Biodiesel to Diesel on the Physical and Chemical Properties and Engine Performance of Fuel Blends." *Journal of Biobased Materials and Bioenergy* 10 (1): 34–43.

[19] Kamil M., Ramadan K., Ghenai C., Olabi A. G., and Nazzal I. T. 2019, "Emissions from Combustion of Second-Generation Biodiesel Produced from Seeds of Date Palm Fruit (*Phoenix Dactylifera L*.)." *Applied Sciences (Switzerland)* 9 (18): 1–24.

[20] Kamil M., Ramadan K.M., Awad O.I., Ibrahim T. K., Inayat A., and Ma X. 2019, "Environmental Impacts of Biodiesel Production from Waste Spent Coffee Grounds and Its Implementation in a Compression Ignition Engine." *Science of the Total Environment* 675: 13–30.

[21] Đurišić-Mladenović N., Kiss F., Škrbić B., Tomić M., Mićić R., and Predojević Z. 2018, "Current State of the Biodiesel Production and the Indigenous Feedstock Potential in Serbia" 81 (June 2017): 280–91.

[22] Krishnakumar U., Sivasubramanian V., and Selvaraju N. 2013, "Physico-Chemical Properties of the Biodiesel Extracted From Rubber Seed Oil Using Solid Metal Oxide Catalysts" *IJERA*. 3 (4): 2206–9.

[23] Liu R.S., Zhang L., Sun X., Liu H., and Zhang J. 2012, "Electrochemical Technologies for Energy Storage and Conversion." *Electrochemical Technologies for Energy Storage and Conversion* 1–2:1-806.

[24] Lowe B., Gardy J., and Hassanpour A. 2022, "The Role of Sulfated Materials for Biodiesel Production from Cheap Raw Materials." *Catalysts*.12, 223: 1-22.

[25] Michen B., Geers C., Vanhecke D., Endes C., Rothen-Rutishauser B., Balog S., and Petri-Fink A. 2015, "Avoiding Drying-Artifacts in Transmission Electron Microscopy: Characterizing the Size and Colloidal State of Nanoparticles." *Scientific Reports* 5: 9793:1-7.

[26] Millinger M., Meisel K., Budzinski M., and Thrän D. 2018, "Competitiveness of Biofuels in Germany," *Energies*. 11(3): 1–23.

[27] Mofijur M., Rasul M.G., Hyde J., Azad A.K., Mamat R., Bhuiya M.M.K. 2016, "Role of Biofuel and Their Binary (Diesel-Biodiesel) and Ternary (Ethanol-Biodiesel-Diesel) Blends on Internal Combustion Engines Emission Reduction." *Renewable and Sustainable Energy Reviews* 53: 265–78.

[28] Mosaddegh E., Hassankhani A., Pourahmadi S., and Ghazanfari D. 2013, "Ball Mill-Assisted Preparation of Nano-CaCO3 as a Novel and Green Catalyst-Based Eggshell Waste: A Green Approach in the Synthesis of Pyrano[4,3-b]Pyrans." *International Journal of Green Nanotechnology* 5 (1): 1–5.

[29] Murray J.W. 2016. "Limitations of Oil Production to the IPCC Scenarios: The New Realities of US and Global Oil Production." *BioPhysical Economics and Resource Quality* 1 (2): 1–13.

[30] Noor C.W.M., Noor M.M., and Mamat R. 2018, "Biodiesel as Alternative Fuel for Marine Diesel Engine Applications: A Review." *Renewable and Sustainable Energy Reviews* 94 (May): 127–42.

[31] Ogunkunle O., and Ahmed N.A. 2019, "A Review of Global Current Scenario of Biodiesel Adoption and Combustion in Vehicular Diesel Engines." *Energy Reports* 5: 1560–79.

[32] Owusu P.A., and Asumadu-Sarkodie S. 2016, "A Review of Renewable Energy Sources, Sustainability Issues and Climate Change Mitigation." *Cogent Engineering* 3 (1): 1–14.

[33] Ozturk I. 2016, "Utilizing Biofuels for Sustainable Development in the Panel of 17 Developed and Developing Countries," *GCB Bioenergy*. 8:4: 826–36.

[34] Perera F. 2018, "Pollution from Fossil-Fuel Combustion Is the Leading Environmental Threat to Global Pediatric Health and Equity: Solutions Exist." *International Journal of Environmental Research and Public Health* 15 (1):17-33.

[35] Raj B., and Singh O. 2012, "Global Trends of Fossil Fuel Reserves and Climate Change in the 21st Century." *Fossil Fuel and the Environment*, Chapter 12, 167-192.

[36] Rodrigues A. Bordado J. C., and Santos R. G. 2017, "Upgrading the Glycerol from Biodiesel Production as a Source of Energy Carriers and Chemicals—A Technological Review for Three Chemical Pathways." *Energies*. 10(11):1817: 1-36.

[37] Virk H. S, and Sharma P. 2010, "Chemical Route to Nanotechnology." *International Journal of Advanced Engineering Technology E-ISSN*. I. (III).114-129.

[38] Seela C.R., Sankar B.R., and Kiran D.S. 2016, "Influence of Biodiesel and Its Blends on CI Engine Performance and Emissions: Influence of Biodiesel and Its Blends on CI Engine Performance and Emissions: A Review," *Biofuels*.1–17.

[39] Brame J., and Griggs C. 2016. "Surface Area Analysis Using the Brunauer- Emmett-Teller (BET) Method Scientific Operating Procedure Series: SOP-C Environmental Laboratory," ERDC/ELSR-16-3.1-17

[40] Supriyanto E., Sentanuhady J., Dwiputra A., Permana A., and Muflikhun M. A. 2021, "The Recent Progress of Natural Sources and Manufacturing Process of Biodiesel: A Review." *Sustainability (Switzerland)* 13 (10).13:5599: 1-26.

[41] Suresh M., Jawahar C.P., and Richard A. 2018, "A Review on Biodiesel Production, Combustion, Performance, and Emission Characteristics of Non-Edible Oils in Variable Compression Ratio Diesel Engine Using Biodiesel and Its Blends." *Renewable and Sustainable Energy Reviews* 92 (March): 38–49.

[42] Sut D., Chutia R.S., Bordoloi N., Narzari R., and Kataki R. 2016, "Complete Utilization of Non-Edible Oil Seeds of Cascabela Thevetia through a Cascade of Approaches for Biofuel and by-Products." *Bioresource Technology* 213: 111–120.

[43] Trinh T.A., and Linh Le T.P. 2018. "Biofuels Potential for Transportation Fuels in Vietnam: A Status Quo and SWOT Analysis." IOP Conf Ser Earth Environ Sci. 143: 1-18.

[44] Ulusoy Y., Arslan R., Tekin Y., Surmen A., Bolat A., and Sahin R. 2018. "Investigation of Performance and Emission Characteristics of Waste Cooking Oil as Biodiesel in a Diesel Engine." *Pet Sci*. 15:396–404.

[45] Dallatu Y.A., Agbaji E.B. and Ajibola V.O. 2017. "The influence of physicochemical characteristics of a non-oil of yellow oleander seed on its fuel properties" *Bajopas*. 10 (2): 283–91.

[46] Yadav A.K., Pal A., Ghosh U., and Gupta S.K. 2017. "Comparative Study of Biodiesel Production Methods from Yellow Oleander Oil and Its Performance Analysis on an Agricultural Diesel Engine." *International Journal of Ambient Energy* 0 (0): 1–18.

[47] Zhou D., Bennett S.W., and Keller A.A. 2012. "Increased Mobility of Metal Oxide Nanoparticles Due to Photo and Thermal Induced Disagglomeration." *PLoS ONE* 7 (5). :1-8.

[48] Zou C., Zhao Q., Zhang G., and Xiong B. 2016. "Energy Revolution: From a Fossil Energy Era to a New Energy Era." *Natural Gas Industry* 36 (1): 1–10.